

The Griffiths ISRU-Powered Plasma Hopper (IMPH) A Shear-Stabilized Electromagnetic Surface Hopper with ISRU Propellant Generation and Kelvin-Helmholtz Bounded Operation

Wayne Griffiths 

Managing Director, Advanced EM Systems LLC, Auckland, New Zealand.

Abstract: The Griffiths ISRU-Powered Plasma Hopper (IMPH) is a disc-shaped surface lander and hopper vehicle designed for planetary exploration on bodies where in-situ resources are accessible at or near the surface. The IMPH harvests local feedstock (CO₂ from the Martian atmosphere, H₂O ice from polar deposits, CH₄ from Titan surface lakes), cracks it via an integrated GNMT microwave power module, generates plasma through electromagnetic confinement coils, and fires a burst-mode plasma plume downward through the electromagnetic edge to execute surface hops of 10 to 500 km range. The architecture eliminates dependence on Earth-supplied propellant: the planetary surface itself is the fuel source. The plasma drive employs shear-stabilized electromagnetic confinement addressing fundamental instability limitations in high-power plasma thrusters. Traditional systems including VASIMR, helicon thrusters, and magnetoplasmadynamic accelerators suffer from Kelvin-Helmholtz instabilities, anomalous cross-field transport, and erosion from plasma-wall interactions. The IMPH resolves these through engineered shear-layer stabilization where controlled velocity gradients create viscous dissipation exceeding instability growth rates, maintaining stable operation without active feedback control or complex magnetic field topologies. The vehicle operates in three modes. Mode A provides low-power plasma conditioning and precision landing at 10 to 50 kW, 5 to 15 N, Isp 1,500 to 2,500 s. Mode B executes primary hop ascent and descent burns at 50 to 200 kW, 20 to 60 N, Isp 2,500 to 3,500 s. Mode C enables high-performance long-range hops at 200 to 500 kW, 60 to 150 N, Isp 3,500 to 5,000 s with Kelvin-Helmholtz stability margins exceeding factors of 3 to 5 over critical thresholds. Mode transitions occur through software control of magnetic field strength, propellant flow rate, and microwave power allocation without hardware reconfiguration.

Table of Contents

1. Introduction.....	1
2. Vehicle Architecture.....	2
3. Tri-Modal Operation	4
4. Plasma Physics and Stability Analysis	5
5. ISRU Propellant System	6
6. Thermal Management.....	7
7. Governing Equations Reference	7
8. Surface Hop Mission Profile and Operational Doctrine	8
9. Mission Applications, Planetary Surface Exploration	9
10. Comparative Analysis, Planetary Surface Mobility.....	10
11. Technology Development Roadmap.....	11
12. Griffiths Canon Integration	11
13. Conclusion	12
14. Conclusion	12
15. References.....	13
16. Conflict of Interest.....	13
17. Funding	13

1. Introduction

Planetary surface exploration is fundamentally constrained by propellant mass. Every kilogram of propellant delivered from Earth consumes launch mass budget that could carry science instruments, power systems, or crew supplies. For surface mobility across distances of tens to hundreds of kilometres, this constraint has historically limited missions to rovers crawling at centimetres per second across terrain that might take years to traverse. The IMPH breaks this constraint by treating the planetary surface as the propellant source. On Mars, atmospheric CO₂ and subsurface H₂O ice are accessible in abundance. On Titan, CH₄ is a surface liquid. On the lunar poles, H₂O ice exists in permanently shadowed craters. The IMPH harvests these resources, cracks the feedstock molecules into plasma-ready gas using the GNMT microwave power module integrated into the vehicle body, and accelerates the resulting plasma through a shear-stabilized electromagnetic nozzle to generate hop propulsion. A single IMPH vehicle can execute indefinite multi-hop surface traversals, limited only by vehicle health and power availability. The vehicle is a member of the Griffiths Canon [1-5], sharing the GNMT microwave power architecture [2] and the electromagnetic field-governance principles applied across Canon systems at all scales. Canon heritage from GNMT,

*Managing Director, Advanced EM Systems LLC, Auckland, New Zealand. **Corresponding Author:** waynegriffiths9@gmail.com.

Article History: Received: 03-April-2026 || Revised: 30-May-2026 || Accepted: 30-May-2026 || Published Online: 05-June-2026.

REMNs, and H2EM subsystem development provides a validated technology foundation that substantially de-risks the IMPH development programme.

Shear Stabilization Principles

Kelvin-Helmholtz instabilities arise when velocity shear exceeds critical thresholds determined by density gradients and magnetic field topology. The linear growth rate scales as γ approximately equal to shear rate squared divided by Alfvén velocity times wavenumber. Viscous damping suppresses perturbations at a rate proportional to viscosity times wavenumber squared. Stability occurs when viscous damping exceeds instability growth rate, achievable when shear length scales are sufficiently short that dissipation dominates inertial effects. The IMPH creates controlled shear through differential propellant injection establishing velocity gradients of 50 to 500 km/s/m over radial scale lengths of 1 to 5 cm. Rather than minimizing gradients or accepting instabilities as performance limitations, the architecture engineers controlled gradients that create viscous dissipation exceeding instability growth rates across the relevant wavenumber spectrum. The Richardson number $Ri = N^2_{BV} / (du/dr)^2$ provides the key stability criterion, with Ri greater than 0.25 to 1.0 indicating stable conditions. IMPH targets $Ri = 0.5$ to 2.5 across all operating modes.

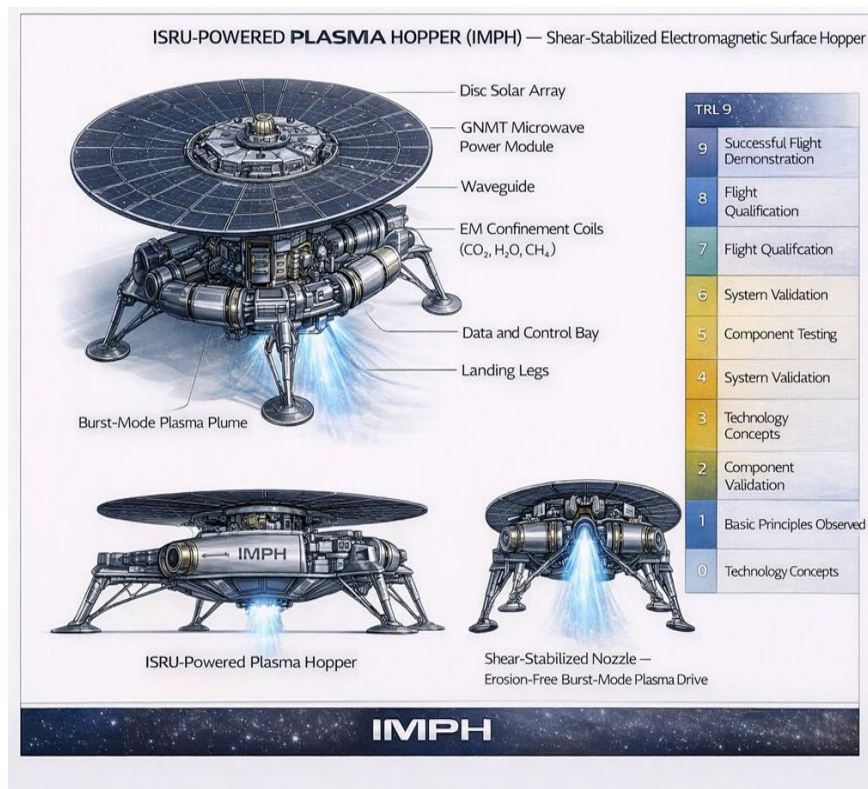


Figure 1. IMPH System Overview, three-view: (top) isometric showing disc solar array, GNMT Microwave Power Module, waveguide, EM confinement coils, ISRU feedstock tanks (CO₂, H₂O, CH₄), data and control bay, landing legs, burst-mode plasma plume; (lower-left) side profile ISRU-Powered Plasma Hopper; (lower-right) shear-stabilized nozzle rear view. TRL pathway inset at right.

2. Vehicle Architecture

The IMPH is a disc-shaped surface lander and hopper vehicle. The large circular solar array disc mounted on top captures power across a wide collection area optimized for low solar flux environments including Mars and outer body missions. The GNMT Microwave Power Module occupies the central hub of the disc, receiving electrical power and outputting microwave energy into the plasma generation chamber below. Electromagnetic confinement coils ring the vehicle mid-body, with ISRU feedstock tanks carrying CO₂, H₂O, and CH₄ integrated into the equatorial body ring. The data and control bay, gas inlets, waveguide, and antenna occupy dedicated bays in the body structure. Four to six landing legs extend outward and downward, terminating in wide footpads optimized for soft, unconsolidated regolith. The burst-mode plasma plume fires downward through the electromagnetic edge at the base of the vehicle.



GNMT Microwave Power Module

The GNMT Microwave Power Module is the power and processing core of the IMPH, directly inherited from the Griffiths Canon nuclear microwave-thermal propulsion architecture [2] and adapted for solar-electric surface applications. The module operates at 13.56 or 27.12 MHz using GaN solid-state amplifiers, accepting electrical power from the solar array and converting it to microwave energy delivered via waveguide into the cracking chamber. Coupling efficiency of 70 to 85 percent has been demonstrated in laboratory helicon sources with similar plasma parameters. Solar array area is sized to deliver 10 to 500 kW depending on solar distance and dust loading, with battery buffering enabling burst-mode operation at peak power levels exceeding average solar input.

ISRU Feedstock System

The ISRU feedstock system extracts, stores, and delivers propellant from planetary surface resources. Three feedstock pathways are baselined. CO₂ extraction from the Martian atmosphere uses molecular sieve adsorption or Sabatier-cycle processing. H₂O ice mining uses resistive heating or microwave energy to sublimate subsurface or surface ice deposits. CH₄ recovery applies to Titan surface operations where liquid methane lakes provide direct feedstock access. All three feedstocks are plasma-compatible when processed through the GNMT cracking chamber. Feedstock purity requirements are relaxed relative to noble gas propellants since molecular dissociation products are intrinsic to ISRU operation, making field processing practical without laboratory-grade purification.

EM Confinement Coils and Shear-Stabilized Nozzle

The electromagnetic confinement coils ring the vehicle mid-body, producing axisymmetric magnetic fields of 300 to 2,000 Gauss depending on operating mode. The field geometry employs controlled divergence creating a magnetic nozzle effect that converts perpendicular plasma thermal energy into directed axial flow. Field strength profiles follow $B(z) = B_0 / (1 + (z/L)^2)$, where B_0 is the throat field and L is the characteristic divergence length. Mirror ratio $R_m = B_{throat} / B_{exit}$ of 10 to 30 achieves thermal-to-kinetic conversion efficiencies of 75 to 85 percent. The shear-stabilized nozzle creates the controlled velocity gradient shear layer through differential propellant injection, an inner high-velocity core surrounded by an outer low-velocity annular region. Velocity transitions occur over 5 to 20 mm radial scale lengths comparable to the ion gyroradius, keeping velocity gradients within the MHD regime. The electromagnetic edge defines the boundary of the authorized plasma exhaust zone. Burst-mode operation fires the plasma plume in controlled pulses timed by the supervisory control system.

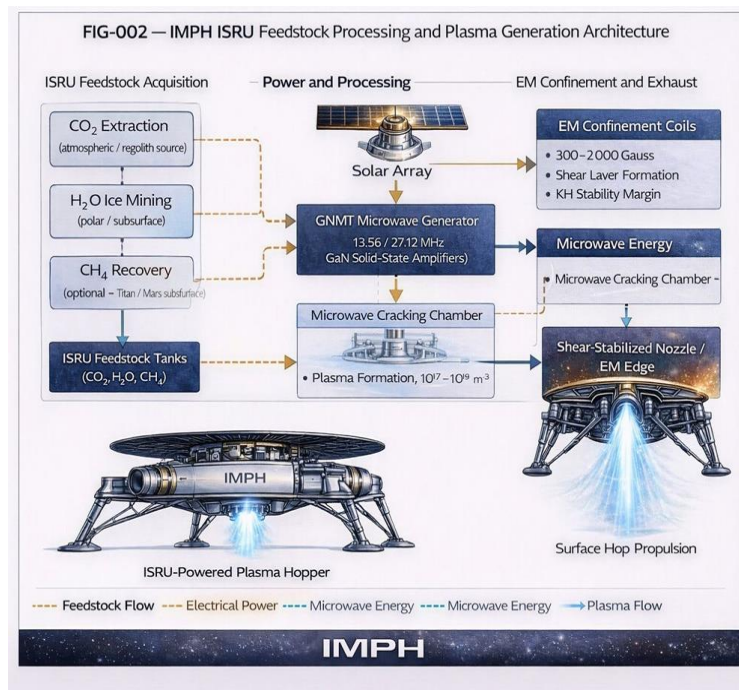


Figure 2 IMPH ISRU Feedstock Processing and Plasma Generation Architecture, feedstock acquisition (CO₂ extraction, H₂O ice mining, CH₄ recovery) feeds ISRU tanks, processed by GNMT Microwave Generator through Microwave Cracking Chamber into EM Confinement Coils and Shear-Stabilized Nozzle/EM Edge for Surface Hop Propulsion. Solar array powers GNMT module throughout.

3. Tri-Modal Operation

The IMPH operates in three modes optimised for different phases of the hop cycle and different mission requirements. Mode selection occurs through software control of magnetic field strength, microwave power level, and propellant flow rate without mechanical reconfiguration.

Table 1. IMPH tri-modal performance summary. All mode transitions through software control only. ISRU feedstock composition affects Isp: CO2 plasma yields lower Isp than noble gas but costs nothing to source on Mars or Titan.

Parameter	Mode A, Conditioning / Landing	Mode B, Primary Hop	Mode C, Long-Range
Electrical input power	10 – 50 kW	50 – 200 kW	200 – 500 kW
Thrust	5 – 15 N	20 – 60 N	60 – 150 N
Specific impulse (Isp)	1,500 – 2,500 s	2,500 – 3,500 s	3,500 – 5,000 s
Thrust-to-power ratio	~0.67 mN/W	~0.36 mN/W	~0.34 mN/W
Magnetic field strength	300 – 800 Gauss (permanent magnets)	800 – 1,500 Gauss (EM coils)	1,500 – 2,000 Gauss (superconducting)
Plasma density	$10^{17} - 10^{18} \text{ m}^{-3}$	$10^{18} - 10^{19} \text{ m}^{-3}$	$\sim 10^{19} \text{ m}^{-3}$
Electron temperature	3 – 5 eV	5 – 8 eV	8 – 12 eV
Propellant flow rate	4 – 10 mg/s	8 – 18 mg/s	15 – 30 mg/s
KH stability margin	5 – 8x critical threshold	3 – 5x critical threshold	2 – 3x critical threshold
Richardson number (Ri)	1.5 – 2.5	0.8 – 1.5	0.5 – 0.8
Thermal load	1.5 – 5 kW (passive radiation)	8 – 50 kW (deployable radiators)	30 – 125 kW (active cooling)
Primary use in hop cycle	Pre-hop conditioning; precision landing retro-burn; attitude trim	Ascent burn; descent burn; standard hops 10–200 km	Long-range hops 200–500+ km; high-gravity-well escape
ISRU feedstock options	CO ₂ , H ₂ O vapour, CH ₄	CO ₂ , H ₂ O, CH ₄ , Ar (carried)	CO ₂ + H ₂ O blend optimal; CH ₄ on Titan

Mode A - Plasma Conditioning and Precision Operations: Mode A is the workhorse of surface operations: pre-hop plasma conditioning, precision landing retro-burn, attitude trim, and short-range repositioning. Conservative magnetic field of 300 to 800 Gauss from permanent magnet assemblies enables operation without superconducting magnets. KH stability margins of 5 to 8 times critical threshold provide robust operation tolerant to variations in ISRU feedstock composition, which will vary with local resource quality and atmospheric conditions.

Mode B - Primary Hop Ascent and Descent: Mode B executes the primary ascent, and descent burns for standard surface hops. At 50 to 200 kW and 20 to 60 N sustained thrust with Isp 2,500 to 3,500 s, Mode B provides the optimal balance of thrust and specific impulse. The ascent burn follows a gravity-turn trajectory from near-vertical liftoff through an arc to the coast phase. Descent burns use a similar profile in reverse, with Mode B providing continuous thrust authority for precision landing site targeting. Shear stabilization margins of 3 to 5 times remain comfortable for sustained operation across the full burn duration.

Mode C - Long-Range and High-Performance Operations: Mode C enables long-range hops requiring maximum delta-v per propellant mass, and operations on bodies with higher surface gravity. At 200 to 500 kW and 60 to 150 N, KH stability margins compress to 2 to 3 times critical threshold, requiring precise control of propellant injection uniformity and magnetic field profiles. Superconducting coils at 1,500 to 2,000 Gauss maintain confinement at high plasma density. Mode C enables planetary-scale surface traversals such as hopping from equatorial science sites to polar ice deposits on Mars in a single mission sequence.



4. Plasma Physics and Stability Analysis

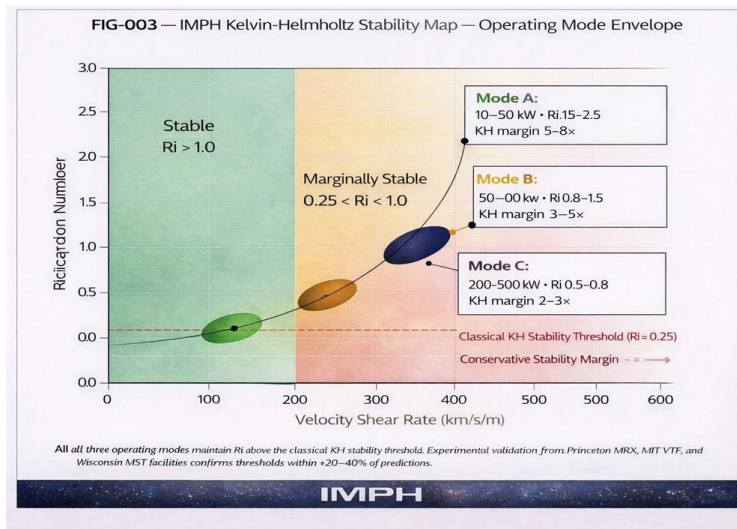


Figure 3 IMPH Kelvin-Helmholtz Stability Map, Richardson number vs. velocity shear rate. Stable region (green, $Ri > 1.0$), marginally stable (amber, $0.25 < Ri < 1.0$), unstable (red, $Ri < 0.25$). Mode A, B, C operating ellipses with power and KH margin annotations. All three modes maintain Ri above the classical KH stability threshold of $Ri = 0.25$.

The theoretical foundation for shear stabilization derives from fluid plasma theory where velocity gradients create viscous stresses that damp perturbations before they amplify into disruptive instabilities. For magnetized plasmas, effective viscosity includes both classical collisional contributions and anomalous turbulent transport, with total viscosity coefficients typically 10 to 100 times classical predictions depending on magnetic field topology and plasma beta.

Table 2. IMPH stability parameters by operating mode. Experimental validation from Princeton MRX, MIT VTF, and Wisconsin MST facilities confirms stability thresholds within +/- 20 to 40 percent of theoretical predictions.

Stability Parameter	Mode A	Mode B	Mode C	Notes
Alfven velocity (v_a)	15 – 20 km/s	20 – 30 km/s	30 – 40 km/s	Scales with $B/\sqrt{\rho}$
Critical Δv threshold	8 – 12 km/s	12 – 20 km/s	20 – 25 km/s	Sets KH instability onset
Actual Δv (injection)	5 – 8 km/s	10 – 18 km/s	30 – 50 km/s	Controlled by injector geometry
Velocity ratio ($\Delta v / v_a$)	0.2 – 0.5	0.5 – 0.8	1.0 – 2.0	$< 1 =$ stable regime target
Richardson number (Ri)	1.5 – 2.5	0.8 – 1.5	0.5 – 0.8	$Ri > 0.25 =$ stable condition
KH stability margin	5 – 8x	3 – 5x	2 – 3x	Factor above critical threshold
Shear layer width	5 – 20 mm	3 – 10 mm	2 – 8 mm	Comparable to ion gyroradius
Shear gradient (dv/dr)	50 – 100 km/s/m	100 – 300 km/s/m	300 – 500 km/s/m	Set by injector manifold

Magnetic Nozzle Physics

Magnetic nozzle physics governs conversion of perpendicular thermal energy into directed axial kinetic energy. Mirror ratio $R_m = B_{throat} / B_{exit}$ of 10 to 30 achieves thermal-to-kinetic conversion efficiencies of 75 to 85 percent. Plasma detachment from magnetic field lines at the nozzle exit occurs through the frozen-flow condition where plasma velocity exceeds Alfven velocity, breaking magnetic flux-freezing and allowing neutral expansion.

For IMPH exit conditions with Alfvén velocity 10 to 30 km/s and exhaust velocity 25 to 50 km/s, detachment occurs reliably. Far-field plume expansion follows self-similar gas-dynamic scaling with divergence half-angle 15 to 30 degrees.

5. ISRU Propellant System

The ISRU propellant system is the defining innovation of the IMPH. By sourcing propellant from the planetary environment, the IMPH transforms the rocket equation for surface mobility: each hop replenishes the propellant expended on the previous hop, enabling indefinite multi-hop traversal limited only by vehicle health and power availability. No Earth-resupply of propellant is required after the initial launch charge.

Table 3. ISRU feedstock options by target body. CO₂ is the baseline Mars propellant due to abundance and extraction simplicity. First-hop propellant is Earth-supplied noble gas; all subsequent hops use ISRU feedstock sourced at the target body.

Target Body	Primary Feedstock	Source	Processing Method	Isp Impact	Notes
Mars (atmosphere)	CO ₂	Atmospheric extraction	Molecular sieve adsorption	Lower than noble gas - ~1,800–2,500 s Mode B	Abundant; extraction power 50–200 W per g/hr
Mars (subsurface)	H ₂ O ice	Subsurface ice mining via drill or microwave sublimation	Electrolysis or direct plasma cracking	H ₂ plasma Isp ~3,000–5,000 s; O ₂ vented	Polar deposits; equatorial subsurface ice confirmed
Mars (combined)	CO ₂ + H ₂ O blend	Both atmospheric and subsurface sources	Sabatier cycle or direct blend	Intermediate Isp; tunable by blend ratio	Direct blend simpler than Sabatier
Moon (polar)	H ₂ O ice	Permanently shadowed crater mining	Microwave sublimation and cracking	H ₂ /O plasma Isp ~3,000–4,500 s	LCROSS/LRO confirmed polar ice deposits
Titan	CH ₄	Surface lake direct collection	Minimal, liquid at surface temperature	CH ₄ plasma Isp ~2,000–3,500 s	Simplest ISRU of all target bodies
Asteroids (C-type)	H ₂ O (hydrated regolith)	Regolith heating and vapour collection	Microwave heating and collection	H ₂ O vapour plasma Isp ~1,800–2,500 s	Resource availability varies by body
Carried (first hop)	Ar or Xe (Earth-supplied)	Onboard tank from launch	None	Ar Isp ~2,500–3,500 s; Xe ~2,000–3,000 s	First hop only; ISRU takes over thereafter



6. Thermal Management

Table 4. Thermal management by operating mode. Surface thermal environment adds challenges do not present in space-based applications: ISRU propellant tanks require heaters during planetary night to prevent feedstock freezing.

Parameter	Mode A	Mode B	Mode C
Electrical input power	10 – 50 kW	50 – 200 kW	200 – 500 kW
Total drive thermal load	1.5 – 5 kW	8 – 50 kW	30 – 125 kW
Radiator type	Passive, metallic surfaces	Deployable panels (C-C facesheets)	Active, heat pipes and pumped loops
Radiator operating temperature	200 – 400 K	400 – 600 K	500 – 700 K
Active cooling required	No	No	Yes, RF windows and SC coil jackets
Surface thermal challenge	ISRU tanks must not freeze during planetary night	Radiator deployment must not conflict with landing legs	Active thermal loop must survive surface dust ingestion

7. Governing Equations Reference

Table 5. Governing equations reference. EQ-07, EQ-11, and EQ-12 are IMPH-specific equations connecting the GNMT solar power input to ISRU cracking rate, hop range, and refuel timeline respectively.

Equation ID	Name	Expression	Physical Meaning
EQ-01	KH linear growth rate	$\gamma \approx (du/dr)^2 / (va \times k)$	Rate of KH instability growth. Suppressed when viscous damping exceeds growth rate.
EQ-02	Richardson number	$Ri = N^2_{BV} / (du/dr)^2$	$Ri > 0.25$ to 1.0 implies stable shear layer. IMPH targets $Ri = 0.5$ to 2.5 .
EQ-03	KH critical velocity (magnetized)	$\Delta v_{crit} = va$ (Alfven velocity)	Alfven velocity replaces surface tension. $\Delta v < va$ implies stable operation.
EQ-04	Magnetic field profile	$B(z) = B_0 / (1 + (z/L)^2)$	Nozzle field geometry. B_0 = throat field; L = divergence length.
EQ-05	Mirror ratio and nozzle efficiency	$Rm = B_{throat} / B_{exit}$; $\eta \approx 1 - 1/Rm$	$Rm = 10$ to 30 gives $\eta = 75$ to 85 percent thermal-to-kinetic conversion.
EQ-06	Helicon dispersion relation	$\omega = k_{par}^2 \times B \times e / (\mu_0 \times \rho \times m_e)$	Plasma density sets wavelength for given frequency and field. Enables compact GNMT antenna.
EQ-07	GNMT cracking energy balance	$P_{mw} \times \eta_{cav} = \dot{n}_{feed} \times H_{diss}$	Connects solar power input to ISRU feedstock dissociation rate. Core IMPH equation.
EQ-08	Thrust	$F = \dot{m} \times v_e + (p_e - p_{inf}) \times A_e$	\dot{m} = ISRU propellant flow; v_e = exhaust velocity; pressure thrust term included.
EQ-09	Specific impulse	$I_{sp} = F / (\dot{m} \times g_0)$	Propellant efficiency in seconds. Depends on feedstock molecular mass and plasma temperature.

EQ-10	Tsiolkovsky delta-v	$\Delta v = I_{sp} \times g_0 \times \ln(m_0/m_f)$	Hop Δv from propellant mass ratio. m_0 = pre-hop mass; m_f = post-burn mass.
EQ-11	Hop range (vacuum approx)	$R_{hop} \approx \Delta v^2 / g_{surface}$	Approximate ballistic range for given Δv on body with surface gravity g .
EQ-12	ISRU replenishment time	$t_{fill} = m_{prop} / (m_{dot_ISRU} \times \eta_{extract})$	Time to refuel one hop charge. m_{dot_ISRU} = extraction rate; $\eta_{extract}$ = ISRU efficiency.

8. Surface Hop Mission Profile and Operational Doctrine

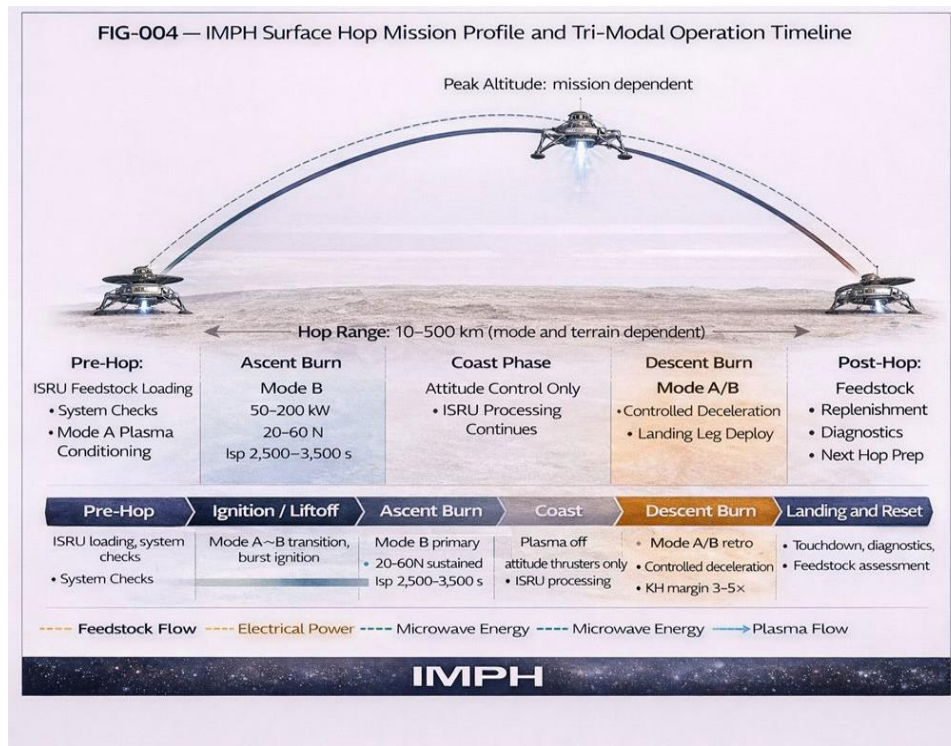


Figure 4 IMPH Surface Hop Mission Profile and Tri-Modal Operation Timeline, hop arc from launch site to landing site (10 to 500 km range) over planetary surface, with five annotated mission phase columns (Pre-Hop, Ascent Burn, Coast Phase, Descent Burn, Post-Hop) and phase timeline strip showing mode assignments and continuous safety layer bands (EM Confinement Active, KH Stability Monitor, ISRU Processing).

This study aimed to assess the adoption readiness and feasibility of electric aircraft for regional air transport in the Philippine archipelago by integrating the Technology Organization Environment (TOE) framework and Diffusion of Innovations (DOI) theory. The results showed that while organizational readiness emerged as the most potent enabler, moderate confidence was expressed regarding technological maturity, and substantial concerns remain regarding infrastructure and regulatory preparedness. DOI analysis confirmed strong perceptions of relative advantage and compatibility, but uncertainty about complexity and limited trial opportunities constrained enthusiasm for adoption. The study makes two key contributions. Theoretically, it extends the application of TOE-DOI models to the emerging field of electric aviation in a developing country context, providing new empirical insights from the Philippine market. The reliability of the survey instrument was also established, with all constructs demonstrating acceptable internal consistency as indicated by Cronbach's Alpha values above 0.70. Practically, it offers evidence-based guidance for regional airlines and regulators on the critical barriers and enablers that must be addressed to support the future integration of electric aircraft.



Table 6. IMPH hop cycle phase sequence. ISRU fill time dominates total cycle time: plasma burn duration is minutes; ISRU replenishment takes hours to days depending on local resource quality and solar power availability.

Phase	Mode	Key Actions	Duration	Safety State
Pre-Hop	A	ISRU feedstock loading complete; system diagnostics; Mode A plasma conditioning; landing leg pre-load check; trajectory solution upload	1 to 72 hours (ISRU fill time dominant)	All systems nominal; abort criteria defined before ignition authorization
Ignition / Ltoff	A to B	Burst ignition; plasma confirmed; thrust vector verified; Mode A to B transition; KH margin monitored continuously	Less than 30 s to stable Mode B	KH margin > 3x required to continue; auto-abort below threshold
Ascent Burn	B	Mode B primary thrust; gravity-turn trajectory; 20 to 60 N sustained; Isp 2,500 to 3,500 s; GNMT at nominal	2 to 15 min hop-range dependent	Continuous KH monitoring; thrust deviation less than 5 percent triggers review
Coast Phase	A off	Plasma off; attitude control thrusters only; ISRU pre-processing of next hop feedstock begins; trajectory correction if required	5 to 120 min range dependent	Attitude hold; abort-to-surface trajectory maintained throughout coast
Descent Burn	A/B	Mode B retro-burn; controlled deceleration; Mode A for final 100 m precision approach; landing leg deploy	2 to 10 min	Landing radar active; abort-to-hover if anomaly detected below 50 m AGL
Post-Hop Reset	A off	Touchdown; system diagnostics; ISRU extraction begins; feedstock quality assessment; science operations; next hop planning	1 to 72 hours (ISRU fill dominant)	Vehicle health assessment; next hop authorized only when tank above 80 percent charge

9. Mission Applications, Planetary Surface Exploration

The IMPH enables a qualitative expansion of planetary surface science reach. Where a conventional rover travels kilometers over months, a single IMPH vehicle can traverse thousands of kilometers across multiple hops, accessing polar ice deposits, deep impact craters, ancient highland terrains, and geologically active regions that would be years away for a wheeled system.

Table 7. IMPH mission applications by target body. All applications use ISRU feedstock sourced at the target body. No Earth-resupply of propellant required after the initial launch charge.

Mission / Target	Feedstock	Mode	Hop Range	Key Capability	Scientific Objective
Mars polar science traverse	H ₂ O ice (polar)	B to C	100 – 500 km per hop	Multi-hop traverse from equatorial landing to polar ice cap	Polar stratigraphy; climate record; water ice resource characterisation
Mars crater floor access	CO ₂ atmospheric	A to B	10 – 50 km	Precision landing in crater floor inaccessible to rovers	Impact melt samples; subsurface exposure; astrobiological targets
Mars multi-site geological survey	CO ₂ + H ₂ O blend	B	50 – 200 km per hop	10+ hop traverse across geological province	Stratigraphic correlation across hundreds of km; resource mapping
Lunar polar ice survey	H ₂ O ice (PSR)	B	50 – 200 km per hop	Access permanently shadowed craters from sunlit charging site	Ice deposit characterisation; ISRU resource assessment for crewed missions
Titan hydrocarbon survey	CH ₄ surface lake	B to C	200 – 500 km per hop	Direct lake access; fill from methane surface; multi-continent survey	Organic chemistry; lake composition; prebiotic molecule inventory
Enceladus/Europa surface access	H ₂ O cryo-vent	A to B	1 – 20 km	Low-gravity precision hopping; vent plume proximity sampling	Active geology; ocean chemistry; biosignature search
C-type asteroid survey	H ₂ O hydrated regolith	A	0.1 – 5 km	Micro-gravity surface hopping; multiple site access in single mission	Carbonaceous chondrite composition; resource inventory; planetary defence

10. Comparative Analysis, Planetary Surface Mobility

Table 8. Comparative analysis of planetary surface mobility architectures. The IMPH is the only system combining multi-hundred-km hop range with ISRU propellant sourcing, enabling unlimited surface traversal on resource-bearing planetary bodies.

System	Mobility Range	Propellant Source	Terrain Access	ISRU Capable	Key Limitation vs IMPH
IMPH (this work)	10 – 500 km per hop; unlimited multi-hop sequence	ISRU: CO ₂ , H ₂ O, CH ₄ from surface	Any terrain, hops over obstacles and chasms	Yes, core architecture	ISRU fill time between hops; power dependency on solar array
Wheeled rover (Perseverance class)	Less than 30 km total mission range	N/A (solar/RTG powered mobility)	Terrain-constrained; cannot cross kilometre-scale obstacles	No	Terrain-limited; slow (100 to 200 m/day); fixed science radius



Chemical hopper (proposed)	50 – 200 km per hop; limited total	Earth-supplied storable propellant	Better than rover; limited by propellant mass	No	Fixed propellant budget; no multi-hop without Earth resupply
Helicopter (Ingenuity class)	Less than 300 m per flight; less than 10 km total	N/A (solar rotorcraft)	Better terrain flexibility than rover; very short range	No	Very short range; less than 1 kg science payload; atmosphere-specific
Ballistic penetrator	Single impact; zero surface mobility	N/A (kinetic delivery)	Subsurface access at impact point only	No	One-way delivery only; no repositioning after impact

11. Technology Development Roadmap

Table 9. IMPH technology development roadmap. Earth-analogue field testing in Phase 3 allows ISRU subsystem validation in Mars-analogue environments before flight commitment.

Phase	Duration	Cost	Key Activities	Success Criteria
Phase 1, Laboratory Demonstration	Months 0 to 12	\$2 to 4M	Demonstrate shear stabilization physics with CO ₂ and H ₂ O feedstocks; characterise GNMT microwave cracking efficiency for ISRU propellants; validate KH stability margins across Mode A/B/C parameters; measure Isp for CO ₂ , H ₂ O, and CH ₄ plasma	Ri > 0.5 in all modes with ISRU feedstocks; GNMT coupling efficiency > 65% for CO ₂ ; Isp within 15% of predictions; KH margin > 3x confirmed
Phase 2, Engineering Model	Months 12 to 24	\$4 to 8M	Full engineering model vehicle; vacuum chamber tethered hop simulation; 200 kW sustained plasma; ISRU extraction system integration; 500+ hour endurance; Mode transition demonstrations; landing leg qualification	Thrust within 10% of prediction; mode transitions less than 60 s; ISRU fill rate meets mission timeline; structural qualification to 10g landing loads
Phase 3, Flight Qualification	Months 24 to 36	\$8 to 15M	Flight unit fabrication; full environmental qualification; Earth-analogue field test (Atacama for CO ₂ ISRU; Arctic for H ₂ O ice); flight demonstration; 5+ hop sequence with ISRU refuelling	Successful autonomous hop sequence; ISRU refuel demonstrated between hops; all KH margins maintained in flight; science delivery to 3+ distinct sites
TOTAL	24 to 36 months	\$14 to 27M	TRL 4 to 5 up to TRL 7 to 8	Multi-hop autonomous surface traversal with ISRU refuelling demonstrated in flight

12. Griffiths Canon Integration

The IMPH is a member of the Griffiths Canon, sharing the GNMT microwave power architecture [2], electromagnetic field-governance principles, and DIGSP supervisory control framework applied across Canon systems. The GNMT Microwave Power Module integrated into the IMPH vehicle body is directly descended from the nuclear microwave-thermal propulsion architecture [2], adapted for solar-electric surface applications. EM confinement coil manufacturing validated for the REMN propulsion nozzle applies directly to IMPH confinement coil

fabrication. DIGSP supervisory control software validated across Canon systems forms the foundation for IMPH autonomous hop sequencing. This shared heritage substantially compresses the IMPH development timeline relative to a clean-sheet design and reduces risk across every subsystem.

13. Conclusion

The Griffiths ISRU-Powered Plasma Hopper (IMPH) presents a surface mobility architecture that fundamentally changes the economics of planetary exploration. By sourcing propellant from the surface environment rather than carrying it from Earth, the IMPH transforms the rocket equation from a constraint into an advantage: larger vehicles with greater science payload and power generation capacity can be landed, because they do not need to carry their traversal propellant mass from Earth. The shear-stabilized electromagnetic plasma drive provides the performance necessary to make ISRU surface hopping practical: Isp of 1,500 to 5,000 s depending on mode and feedstock; sustained operation across hundreds of hours of hop cycles; and KH stability margins of 2 to 8 times critical threshold maintained across all modes. The tri-modal architecture enables a single vehicle design to execute precision landings, standard surface traversals, and continent-spanning hops within a single mission. All subsystems employ flight-proven or laboratory-demonstrated technologies with clear manufacturing pathways. The \$14 to 27M development programme progresses systematically from laboratory physics through Earth-analogue field testing to planetary flight demonstration. Canon heritage from GNMT, REMN, and H2EM subsystem development provides a validated technology foundation that substantially de-risks the programme. The IMPH is not an incremental improvement to surface mobility: it is a new operational tier that makes planetary-scale science reach accessible within a single mission lifetime.

14. Conclusion

This study aimed to assess the adoption readiness and feasibility of electric aircraft for regional air transport in the Philippine archipelago by integrating the Technology Organization Environment (TOE) framework and Diffusion of Innovations (DOI) theory. The results showed that while organizational readiness emerged as the most potent enabler, moderate confidence was expressed regarding technological maturity, and substantial concerns remain regarding infrastructure and regulatory preparedness. DOI analysis confirmed strong perceptions of relative advantage and compatibility, but uncertainty about complexity and limited trial opportunities constrained enthusiasm for adoption. The study makes two key contributions. Theoretically, it extends the application of TOE-DOI models to the emerging field of electric aviation in a developing country context, providing new empirical insights from the Philippine market. The reliability of the survey instrument was also established, with all constructs demonstrating acceptable internal consistency as indicated by Cronbach's Alpha values above 0.70. Practically, it offers evidence-based guidance for regional airlines and regulators on the critical barriers and enablers that must be addressed to support the future integration of electric aircraft.



15. References

- [1] Griffiths, W. (2026). The Griffiths dual-ring superconducting artificial-gravity habitat architecture. *Acceleron Aerospace Journal (AAJ)*, 6(2), 1696–1706.
- [2] Griffiths, W. (2026). Nuclear microwave-thermal propulsion: Megawatt-class NM with rotating electromagnetic nozzles. *Acceleron Aerospace Journal (AAJ)*, 6(2), 1707–1713.
- [3] Griffiths, W. (2026). Electro magnetic curvature theory—Working summary. *Acceleron Aerospace Journal (AAJ)*, 6(2), 1714–1722.
- [4] Griffiths, W. (2026). EM-driven underwater power generation plants (EM-UPGPs). *Acceleron Aerospace Journal (AAJ)*, 6(2), 1723–1732.
- [5] Griffiths, W. (2026). The Griffiths free-flying EVA logistics sled (NGLS). *Acceleron Aerospace Journal (AAJ)*, 6(2), 1733–1744.
- [6] Griffiths, W. (2026). H2EM-field burner: An electromagnetically governed hydrogen combustion system for stable, on-demand thermal applications. AEMS LLC / Zenodo. <https://doi.org/10.5281/zenodo.19332174>
- [7] Chen, F. F., & Boswell, R. W. (1997). Helicon plasma sources. *IEEE Transactions on Plasma Science*, 25(6), 1245–1257.
- [8] Ahedo, E., & Merino, M. (2010). Two-dimensional supersonic plasma acceleration in a magnetic nozzle. *Physics of Plasmas*, 17(7), 073501.
- [9] Choueiri, E. Y. (2009). A critical history of electric propulsion: The first 50 years. *Journal of Propulsion and Power*, 20(2), 193–203.
- [10] Goebel, D. M., & Katz, I. (2008). *Fundamentals of electric propulsion: Ion and Hall thrusters*. Wiley.
- [11] Freidberg, J. P. (2007). *Plasma physics and fusion energy*. Cambridge University Press.
- [12] Chandrasekhar, S. (1961). *Hydrodynamic and hydromagnetic stability*. Oxford University Press.
- [13] Gilmore, D. G. (2002). *Spacecraft thermal control handbook*. The Aerospace Press.
- [14] NASA Mars Exploration Program. (2023). *Mars ISRU technology development (JPL Technical Report)*.
- [15] Longmier, B. W., et al. (2014). Improved efficiency and throttling range of the VX-200 magnetoplasma thruster. *Journal of Propulsion and Power*, 30(1), 123–132.

16. Conflict of Interest

The author declares no competing conflict of interest.

17. Funding

N This research received no external funding. The work was conducted independently by the author without financial support from any public, private, or institutional funding body.